Research article

Journal of MASS SPECTROMETRY

Received: 2 September 2014 Revised: 15 October 2014 Accepted: 12 November 2014 Published online in Wiley Online Library

(wileyonlinelibrary.com) DOI 10.1002/jms.3545

Studies on the collision-induced dissociation of adipoR agonists after electrospray ionization and their implementation in sports drug testing

Josef Dib,[a] Nils Schlörer,[b] Wilhelm Schänzer[a] and Mario Thevis[a,c]*

AdipoR agonists are small, orally active molecules capable of mimicking the protein adiponectin, which represents an adipokine with antidiabetic and antiatherogenic effects. Two adiponectin receptors were reported in the literature referred to as adipoR1 and adipoR2. Activation of these receptors stimulates mitochondrial biogenesis and results in an improved oxidative metabolism (via adipoR1) and increased insulin sensitivity (via adipoR2). Hence, adipoR agonists are potentially performance enhancing substances and targets of proactive and preventive anti-doping measures. In this study, two adipoR agonists termed AdipoRon and 112254 as well as two isotopically labeled internal standards (ISTDs) were synthesized in three-step reactions. The products were fully characterized by nuclear magnetic resonance spectroscopy (NMR), mass spectrometry (MS) and density functional theory (DFT) computation. Collision-induced dissociation pathways following electrospray ionization were suggested based on the determined elemental compositions of product ions, comparison to product ions derived from labeled analogs (ISTDs), H/D-exchange experiments and the results of DFT calculations. The most abundant product ions were found at *m/z* 174, tentatively assigned to protonated 1-benzyl-1,2,3,4-tetrahydropyridine for AdipoRon, and *m/z* 207, suggested as protonated 1-(4-methoxybenzyl)piperazine, for 112254. Notably, the loss of the heterocyclic ring (*i.e.* piperazine and piperidine, respectively) in a supposedly intramolecular elimination reaction was observed in both cases. A qualitative determination of both AdipoR agonists in human plasma was established and fully validated for doping control purposes. Validation items such as recovery (86–89%), specificity, linearity, lower limit of detection (1 ng/ml), intraday (3–18%) and interday (5–16%) precision as well as ion suppression or enhancement were determined. Based on these findings adipoR agonists can be implemented in sports drug testing procedures.

Keywords: doping; sport; mass spectrometry; HRMS; mitochondrial biosynthesis

Introduction

Adiponectin is a protein secreted exclusively in adipocytes. The structure, containing a collagen-like domain and a globular domain, is similar to the complement factor C1q.[1–4] Plasma concentrations of monomeric adiponectin were reported to range from 1.9 to 17 μg/ml.[5] Yamauchi *et al.* demonstrated binding affinities of adiponectin to two receptors referred to as adipoR1 and adipoR2. AdipoR2 is abundantly expressed in liver cells. AdipoR1, however, while ubiquitously expressed, is found mainly in skeletal muscle cells.[6]

Adiponectin has antidiabetic and antiatherogenic effects. In mice, the plasma level of adiponectin is decreased in obesity leading to insulin resistance and type 2 diabetes,[7–9] which is ameliorated by the replenishment of adiponectin. The substrate acts via two major pathways. One relies on the stimulation of the peroxisome proliferator-activated receptor alpha (PPARα) in liver and skeletal muscle (through adipoR2) which leads to an increased insulin sensitivity.[8] The second pathway operates via adipoR1 and the activation of 5′ adenosine monophosphate-activated protein kinase (AMPK).[10–12] Adiponectin increases the concentration of AMP in the muscle, which leads to the increased activity of AMPK.[10] Another effect of adiponectin binding to adipoR1 is the influx of extracellular Ca^{2+} into the cell. These effects lead to an increased mitochondrial biogenesis and improved oxidative metabolism in skeletal muscle. In sum, adipoR1 activated by adiponectin is an exercise-mimetic for muscle cells,[13] indicating adiponectin's potential as a doping agent. This conclusion is supported by two patents published in 2013, which aim at finding adipoR-agonists for adipoR1 and the pseudo-exercise effect these agonists might have.[14,15] The screening studies made by this group were focused on the ability of a molecule to activate AMPK. The most effective hit in this study is named AdipoRon (**1**). A second, less active hit was termed 112254 (**2**). AdipoRon (**1**) and 112254 (**2**) are small, orally active molecules, which act as adiponectin mimetics. Due to its substantially higher activity, most subsequent studies were restricted to AdipoRon (**1**). Treatment of C2C12 myotubes with concentrations of 5–50 μM increases the phosphorylation of AMPK, the expression of PGC-1α and the mitochondrial DNA content in a dose dependent manner. In mice, oral administrated AdipoRon

* *Correspondence to: Mario Thevis, Institute of Biochemistry—Center for Preventive Doping Research, German Sport University Cologne, Am Sportpark Müngersdorf 6, 50933 Cologne, Germany. E-mail: thevis@dshs-koeln.de*

a *Center for Preventive Doping Research—Institute of Biochemistry, German Sport University Cologne, Am Sportpark Müngersdorf 6, 50933, Cologne, Germany*

b *Department of Chemistry, Institute of Organic Chemistry, University of Cologne, Greinstr. 4, 50939, Cologne, Germany*

c *European Monitoring Center for Emerging Doping Agents, Cologne/Bonn, Germany*

(50 mg/kg^{-1} body weight) leads to a maximal plasma concentration of 11.8 μM (5.1 mg/ml^{-1}). It activates both the adipoR1-AMPK-PGC-1α- and adipoR2-PPAR-α-pathway,[16,17] similar to other drugs and drug candidates banned in sports by the Prohibited List of the World Anti-Doping Agency (WADA) as for instance AICAR.[18]

Hence, AdipoRon (**1**), 112254 (**2**) and two isotopically labeled analogs (**3** and **4**, respectively, Fig. 1) used as internal standards (ISTD) were synthesized and characterized by nuclear magnetic resonance spectroscopy (NMR) and high-resolution/high-accuracy tandem mass spectrometry (MS/MS). Furthermore, a fully validated test method, including specificity, lower limit of detection (LLOD), identification capability, robustness, carryover, matrix interferences, recovery, interday and intraday precision and linearity was established for human plasma employing liquid chromatography-tandem mass spectrometry (LC/MS/MS).

Experimental

Chemicals, reagents and plasma samples

All chemicals were commercially available and were used without further purification. 1-Hydroxybenzotriazole hydrate (99%), sodium methanolate (0.5 N in methanol), *N*-(3-dimethylaminopropyl)-*N*′-ethylcarbo-diimide hydrochloride (99%), 4-amino-1-benzylpiperidine (98%), β-alanine methyl ester hydrochloride (98%), 4-hydroxybenzophenone (98%), 1-(4-methoxybenzyl)piperazine (97%), piperazine-2,2,3,3,5,5,6,6-d_8 dihydrochloride (98 atom% D, 98%), 1-(chloromethyl)-4-methoxybenzene (98%) and ethyl bromoacetate-2-^{13}C (99 atom% ^{13}C, 98%), methyl bromoacetate (97%) and triethylamine (99%) were purchased from Sigma-Aldrich (Taufkirchen, Germany). Sodium hydroxide (99%) and 4-*tert*-butylbenzoic acid (99%) were obtained from Merck (Darmstadt, Germany). All solvents used (methanol, dimethylacetamide, *N*,*N*-dimethylformamide, dichloromethane and tetrahydrofurane) were of analytical grade and were used without further purification.

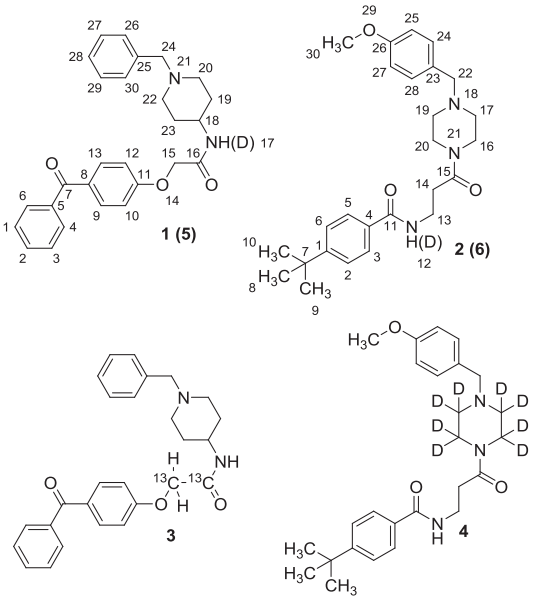

Figure 1. Chemical structures of AdipoRon (**1**, M = 428 g/mol^{-1}), 112254 (**2**, M = 437 g/mol^{-1}), $^{13}C_2$-labeled AdipoRon (**3**, M = 430 g/mol^{-1}) and D_8-labeled 112254 (**4**, M = 446 g/mol^{-1}). Numbers in brackets indicate deuterated AdipoRon (**5**, M = 429 g/mol^{-1}) and 112254 (**6**, M = 438 g mol^{-1}) as obtained by H/D-exchange experiments.

Deionized water used for synthesis and sample preparation was of MilliQ quality. For validation (except specificity), commercially available plasma obtained from Octapharma GmbH (Langenfeld, Germany) was used. For specificity, plasma samples were obtained from healthy volunteers without known medications.

Synthesis and characterization

Synthesis of AdipoRon and $^{13}C_2$-labeled AdipoRon

AdipoRon was synthesized in a three-step reaction (Scheme 1). First a nucleophilic substitution of 4-hydroxybenzophenone (**a**) and methyl bromoacetate (**b**) was conducted to yield methyl 2-(4-benzoylphenoxy)-acetate (**c**). Compound **c** was then saponified to obtain 2-(4-benzoylphenoxy)-acetic acid (**d**). Finally, **d** and 1-benzylpiperidin-4-amine (**e**) were converted to AdipoRon (**1**) by amide formation with 1-hydroxybenzotriazole hydrate (HOBt) and *N*-(3-dimethylaminopropyl)-*N*′-ethylcarbo-diimide hydrochloride (EDCl) as coupling reagents and triethylamine (TEA) as base. The synthesis of the ISTD **3** was performed analogously, but $^{13}C_2$-labeled ethyl bromoacetate was used instead of methyl bromoacetate (**b**).

Synthesis of 112254 and D_8-labeled 112254

The synthesis of 112254 was also a three-stage synthesis (Scheme 1). At first, an amide formation between 4-*tert*-butylbenzoic acid (**f**) and β-alanine methyl ester hydrochloride (**g**) with HOBt and EDCl as coupling reagents and TEA as a base gave methyl 3-(4-(*tert*-butyl)-benzamido)-propanoate (**h**). This was saponified to obtain 3-(4-(*tert*-butyl)-benzamido)-propanoic acid (**i**) followed by the formation of an amide between **i** and the piperazine-derivate **j** yielding the desired product 112254 (**2**). The synthesis of ISTD **4** was conducted accordingly but using a labeled piperazine-derivative prepared via nucleophilic substitution reaction from piperazine-2,2,3,3,5,5,6,6-d_8 dihydrochloride and 1-(chloromethyl)-4-methoxybenzene.

Characterization

The structure of compound **1** and **2** was confirmed by NMR ^{1}H-, H,H-COSY-, H,C-HMQC- and ^{13}C-ATP experiments. Spectra were recorded employing a Bruker Avance III 500 instrument (Bruker, Karlsruhe, Germany) equipped with a 5-mm inverse probe head (z-gradient coil). The spectra were recorded at room temperature from solutions at concentration levels of approximately 10 mg/ml. The elemental composition and dissociation patterns of the substances were determined using high-resolution/high-accuracy mass spectrometry using a LTQ Orbitrap (Thermo, Bremen, Germany). Detailed information and further parameters are described below.

Stock and working solutions

All stock solutions were prepared with a concentration of 1 mg/ml in acetonitrile and stored at −8 °C. Over a period of four weeks no degradation was observed. Working solutions for validation purposes were prepared freshly at the required concentrations by dilution of stock solutions.

Density functional theory calculations

DFT calculations were carried out to determine the most probable position of protonation of compounds **1** and **2**. Preoptimization was conducted for all compounds by MM2 force field calculations.[19] Then, all computations were performed with ORCA freeware (version 2.9.1)[20] at the PBE[21]/def2-TVZP[22] level of theory. All structures were fully optimized, and proton affinities were

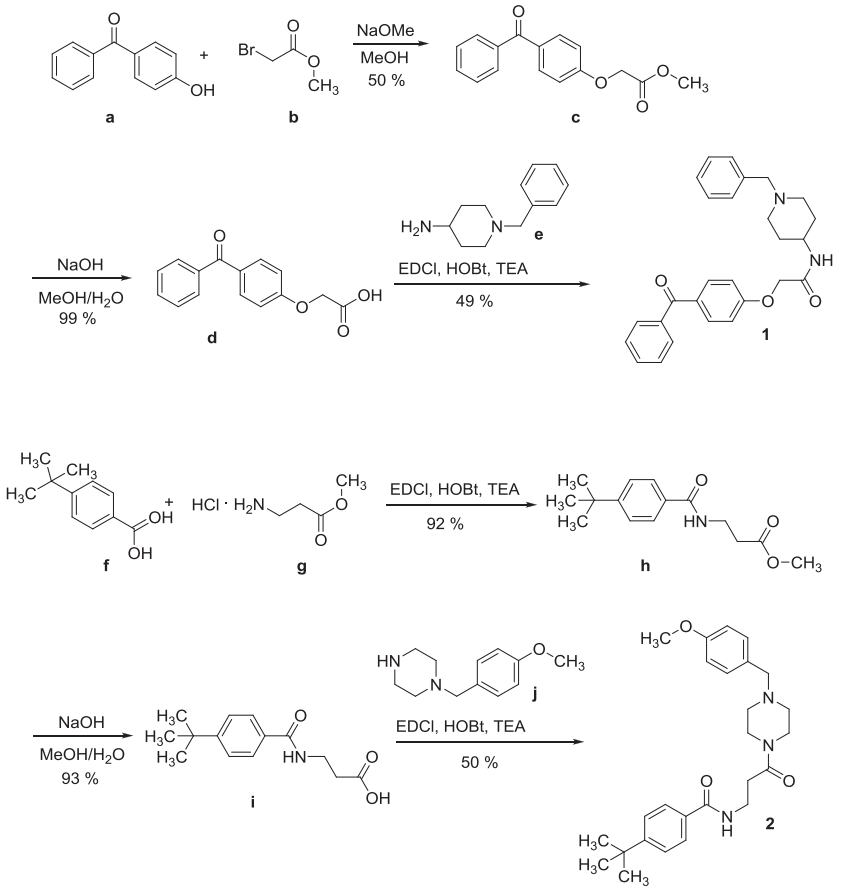

Scheme 1. Route of synthesis of AdipoRon (**1**) and 112254 (**2**).

calculated as the difference between the total energy of the protonated species and the neutral compound. Thermal and vibrational contributions were not considered during computation as they were expected to play a minor role in calculating relative rather than absolute proton affinities.

Electrospray ionization-tandem mass spectrometry and MS^3-experiments

ESI-MS(/MS) and MS^3-experiments were performed on a LTQ Orbitrap mass spectrometer. The instrument, using a HESI-I (heated electrospray ionization-I) source, was operated in positive ionization mode. For calibration, the manufacturer's calibration mixture, consisting of caffeine, the tetrapeptide MRFA and ultramark (mixture of fluorinated phosphazenes), was used. Compounds were introduced into the mass spectrometer via syringe pump at a flow rate of 15 µl/min. They were dissolved in acetonitrile/water (1:1, *v/v*) and at concentrations of 1 µg/ml. Ionization voltage was 5000 V, and the capillary temperature was set to 275 °C. Protonated precursors were isolated using a width of 1.0 Da in the MS^n experiments, and the protonated species were dissociated at normalized collision energies between 20 and 25 (arbitraty units, Xcalibur software version 2.0, Bremen, Germany). For high-resolution mass spectrometry (HRMS), a full width at half maximum (FWHM) of 30 000 (at *m/z* 400) was used, and mass accuracies <5 ppm were accomplished for the period of analysis. Damping gas in the linear ion trap was helium (purity grade 5.0), and gas supplied to the curved linear ion trap (CLT) was nitrogen, obtained from a CMC nitrogen generator (CMC Instruments, Eschborn, Germany)

Liquid chromatography-tandem mass spectrometry

All analyses were performed using an Agilent 1290 Infinity liquid chromatograph linked to an Agilent 6550 iFunnel QTOF LC/MS with electrospray ionization (Waldbronn, Germany). The column used was a Thermo Scientific C_8 Hypersil Gold (100 × 2.1 mm, 3 µm particle size). The eluents were water (mobile phase A) and acetonitrile (mobile phase B), both containing 0.1% formic acid. Gradient elution was employed and started at 2% B increasing to 100% B within 6 min, maintained for 1 min and followed by re-equilibration at 2% B for 3 min. The flow rate was set to 250 µl/min during chromatography and 400 µl/min during re-equilibration. The ion source was operated in positive mode with a temperature of 290 °C, and the spray voltage was 3500 V. The FWHM was 18 000 (at *m/z* 400). Both compounds and the ISTD (**1** to **4**) were detected by means of characteristic product ions formed from protonated molecules by collision-induced dissociation (CID). Nitrogen was used as sheath and collision gas delivered from CMC nitrogen generator (CMC Instruments, Eschborn, Germany).

Sample preparation

Ten microliters of a 0.1 µg/ml^{-1} solution containing both ISTDs was placed in a 1.5-ml polypropylene tube, and the solvent was removed under reduced pressure. Then, 100 µl of plasma was added, followed by the addition of 100 µl of water and 400 µl of acetonitrile. The sample was gently mixed. Precipitated proteins were removed by centrifugation for 5 min at 17 000 *g*. The supernatant was transferred and evaporated under reduced pressure. The

residue was dissolved in 100-µl acetonitrile/water (2:8 *v:v*). The solution was transferred to a HPLC vial, and an aliquot of 10 µl was injected into the LC/MS-system.

H/D-exchange experiments

In order to provide more information for the product ion characterization and dissociation pathways via mass spectrometry, hydrogen/deuterium-exchange experiments were performed for AdipoRon (**1**) and 112254 (**2**). Ten microliters of the stock solution was dissolved in 1 ml of D_2O. After incubation at RT for 3 h, a solution of the deuterated compounds (Fig. 1, **5**, **6**) with the concentration of 1 ppm in acetonitrile/D_2O (1:1 *v:v*) was prepared and introduced into the LTQ Orbitrap mass spectrometer via the syringe pump. The measurements were done under identical conditions as applied to the compounds **1** and **2** without H/D-exchange.

Assay validation

The qualitative determination of the two AdipoR agonists **1** and **2** was validated regarding specificity, LLOD, identification capability, robustness, carryover and matrix interferences according to the International Standard for Laboratories (ISL) of the WADA for non-threshold substances[23] and the WADA technical document with identification criteria for qualitative assays.[24] Additionally, recovery, interday and intraday precision and linearity were determined.

Specificity

Ten plasma samples (five male und five female donors) were prepared as described above at 50 ng/ml to probe for interfering peaks in the ion chromatograms for analyte **1** and **2**.

Lower limit of detection

The LLOD was defined as the 'lowest content that can be measured with a responsible statistical certainty'[25] at a signal-to-noise ratio ≥3. Six plasma samples were fortified with 1 ng/ml of analyte **1** and **2** providing the data to determine the LLOD.

Identification capability

Following the WADA technical document with identification criteria for qualitative assays, the retention time of the analyte shall not differ more than ±0.1 min from that of the same substance.[24] To determine this, six plasma samples fortified with both analytes (50 ng/ml) were analyzed.

Robustness

In order to determine the robustness of the established methodology, six plasma samples fortified with all analytes at 50 ng/ml were prepared as described. The subsequent analyses were conducted using a Thermo Scientific C_8 Accucore X2 (100 × 3 mm, 4 µm particle size).

Carryover

The carryover was determined by analyzing six blank samples between samples fortified with 1, 50 and 200 ng/ml.

Matrix interference

To estimate matrix effects causing ion suppression or enhancement, four plasma samples and four samples with solvent (acetonitrile:water, 8:2, *v/v*), fortified with both compounds **1** and **2**, were prepared (50 ng/ml) and analyzed. The ion suppression was calculated by mean peak area ratios of plasma samples and samples with solvent only.

Recovery

The loss of target compounds during sample preparation was determined by calculating the recovery. Therefore, six samples were fortified with the target analytes at 50 ng/ml before, and another set of samples after preparation of the specimens. To both sample batches, the ISTDs **3** and **4** were spiked at the end of the precipitation protocol. Recoveries were calculated by the mean peak area ratios of the compound and the corresponding ISTD.

Intraday and interday precision

Within one day (intraday) as well as on three consecutive days (interday), six plasma samples of compound **1** and **2** of low (1 ng/ml), medium (50 ng/ml) and high (200 ng/ml) concentration ($n = 54$) were prepared and analyzed. Both intraday and interday precision were calculated for each concentration level.

Linearity

Linearity was tested with six fortified plasma samples at the concentration levels 1, 10, 50, 100, 200 and 300 ng/ml.

Results and discussion

Characterization of adipoR agonists

The overall yields for the synthesis of compounds **1** to **4** range from 24% to 56% (Scheme 1). Only AdipoRon (**1**) and 112254 (**2**) were characterized by NMR spectroscopy, since the labeled compounds **3** and **4** were prepared analogously. The experimental data found for AdipoRon (**1**) and 112254 (**2**) are consistent with the expected chemical shifts and coupling constants and confirm the structures:

*AdipoRon (**1**)*

^{1}H-NMR (500 MHz, $CDCl_3$) δ = 7.97 (s, 1H, H17), 7.81 (d, *J* = 8.7 Hz, 2H, H9, H13), 7.71 (d, *J* = 7.1 Hz, 2H, H1, H3), 7.54 (t, *J* = 7.4 Hz, 1H, H2), 7.44 (t, *J* = 7.6 Hz, 2H, H4, H6), 7.33–7.26 (m, 2H, H27, H29), 7.24–7.13 (m, 2H, H26, H30), 6.95 (d, *J* = 8.8 Hz, 2H, H10, H12), 6.34 (d, *J* = 8.0 Hz, 1H, H28), 4.50 (s, 2H, H15), 3.93–3.84 (m, 1H, H18), 3.46 (s, 2H, H24), 2.77 (d, *J* = 10.8 Hz, 2H, H22), 2.11 (t, *J* = 11.0 Hz, 2H, H20), 1.89 (d, *J* = 10.6 Hz, 2H, H23), 1.57–1.43 (m, 2H, H19) ppm; ^{13}C-NMR (126 MHz, $CDCl_3$) δ = 195.71 (C7), 167.00 (C16), 160.80 (C11), 138.27 (C5, C8), 133.06 (C9, C13), 132.58 (C6, C4), 132.00 (C25), 130.16 (C1, C3), 129.46 (C2, C28), 128.68 (C30), 128.65 (C26), 127.50 (C29), 127.46 (C27), 114.66 (C12, C10), 67.70 (C15), 63.36 (C24), 52.48(C20, C22), 46.68 (C18), 32.48 (C19, C23) ppm.

*112254 (**2**)*

^{1}H NMR (500 MHz, $CDCl_3$) δ = 7.71 (d, *J* = 8.4 Hz, 2H, H3, H5), 7.42 (d, *J* = 8.4 Hz, 2H, H2, H6), 7.20 (d, *J* = 8.5 Hz, 2H, H24, H28), 6.85 (d, *J* = 8.6 Hz, 2H, H25, H27), 3.79 (s, 3H, H30), 3.76–3.70 (m, 2H, H20), 3.63–3.61 (br, 2H, H16), 3.44 (br, 2H, H13), 3.43–3.40 (m, 2H, H22), 2.60 (t, *J* = 5.5 Hz, 2H, H14), 2.42–2.36 (m, 4H, H17, H19), 1.32 (s, 9H, H8–10) ppm; ^{13}C NMR (126 MHz, $CDCl_3$) δ = 170.15 (C16), 167.14 (C11), 158.90 (C4), 154.83 (C1, C23), 131.61 (C26), 130.32 (C24, C28), 126.83 (C3, C5), 125.40 (C2, C6), 113.70 (C25, C27), 62.19 (C14), 55.26 (C30), 52.79 (C19), 52.50 (C17), 45.28 (C22), 41.56 (C16), 35.46 (C20), 34.89 (C7), 32.79 (C17), 31.18 (C8–10) ppm.

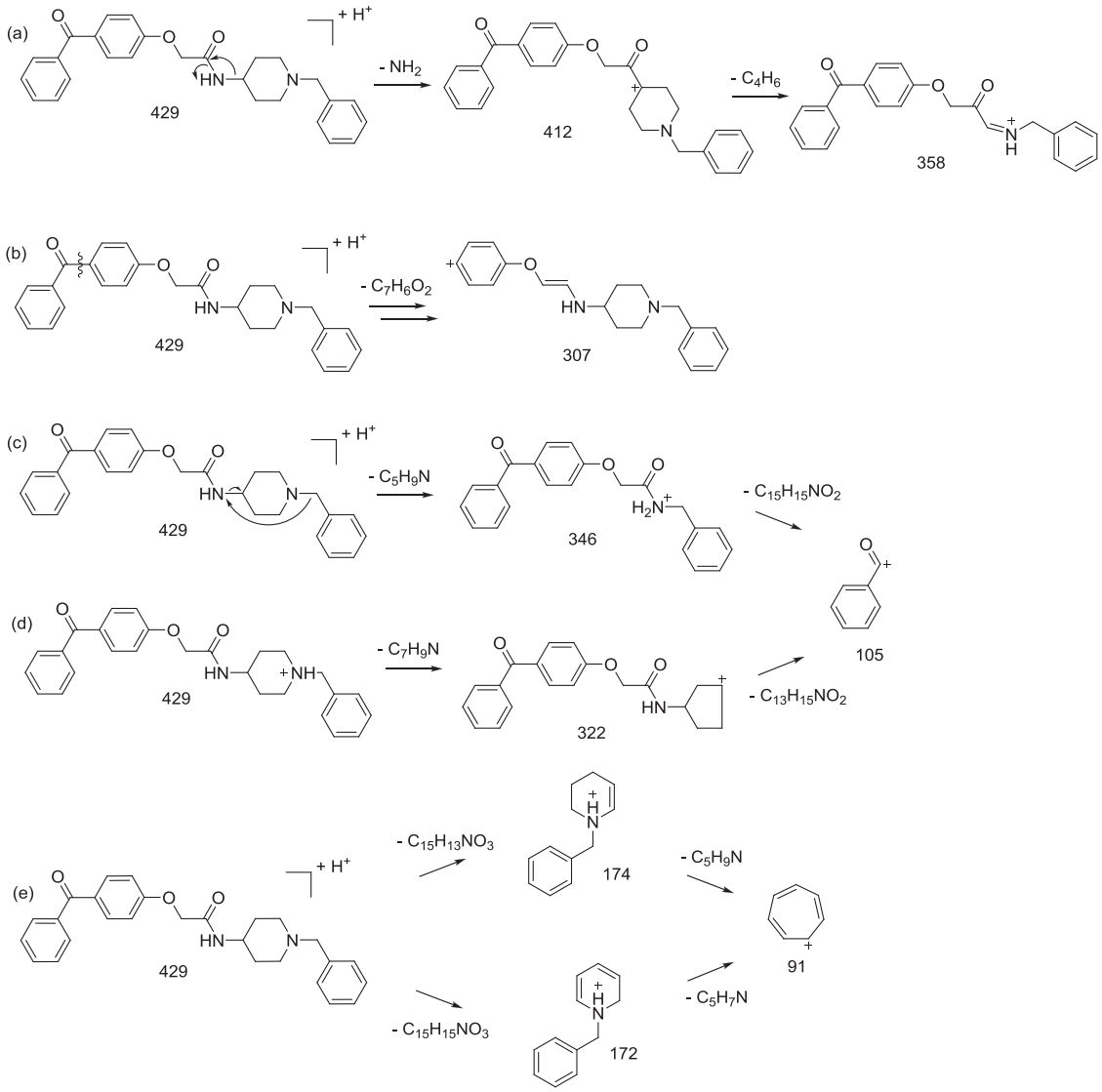

Scheme 2. Proposed dissociation pathway of AdipoRon (**1**).

Electrospray ionization-tandem mass spectrometry

The CID behavior of compounds **1** to **6** was studied using high-resolution/high accuracy (tandem) mass spectrometry using a hybrid linear ion trap-orbitrap system. Product ion mass spectra of synthesized compounds are illustrated in Fig. 2, and accurate masses and calculated elemental compositions of precursor and product ions are listed in Table 1. Proposed dissociation pathways for the protonated molecules of AdipoRon (**1**) and 112254 (**2**) are depicted in Schemes 2 and 3, substantiated by stable isotope labeling (compound **3** and **4**) and H/D-exchange experiments (compound **5** and **6**).

*AdipoRon (**1**)*

According to DFT calculations, the highest proton affinity of AdipoRon (**1**) is given at position 21 (Fig. 1), namely the nitrogen of the piperidine-system, which is favored by 76 kJ/mol^{-1} over the oxygen at position 16. The resulting equilibrium structure is shown in Fig. 3a.

Dissociation of the protonated molecule of **1** under given CID conditions yields the most abundant product ion at *m/z* 174 (Fig. 2a), which is suggested to represent the protonated species of 1-benzyl-1,2,3,4-tetrahydropyridine (Scheme 2e). Both *m/z* 174 and *m/z* 172, tentatively assigned to protonated 1-benzyl-1,2-dihydropyridine, further dissociate to the ion at *m/z* 91, which is proposed to consist of a cycloheptatrienyl cation, generated by the elimination of the respective partially hydrated pyridine systems (−83 u and −81 u) as corroborated by MS^3 experiments (Scheme 2e).

The product ion at *m/z* 307 nominally results from the loss of benzoic acid (122 u) from the protonated molecule of **1**. Its generation remains unclear; however, $^{13}C_2$-labeling (compound **3**, Fig. 2c) and H/D-exchange experiments (compound **5**, Fig. 2e) indicate the presence of both ^{13}C-labels (*m/z* 309) and one deuterium in the product ion. Hence, a complex intramolecular rearrangement is required that arguably involves the benzoyl moiety (carbons 1–7) and the amide oxygen at C-16, suggesting a product ion structure as proposed in Scheme 2c.

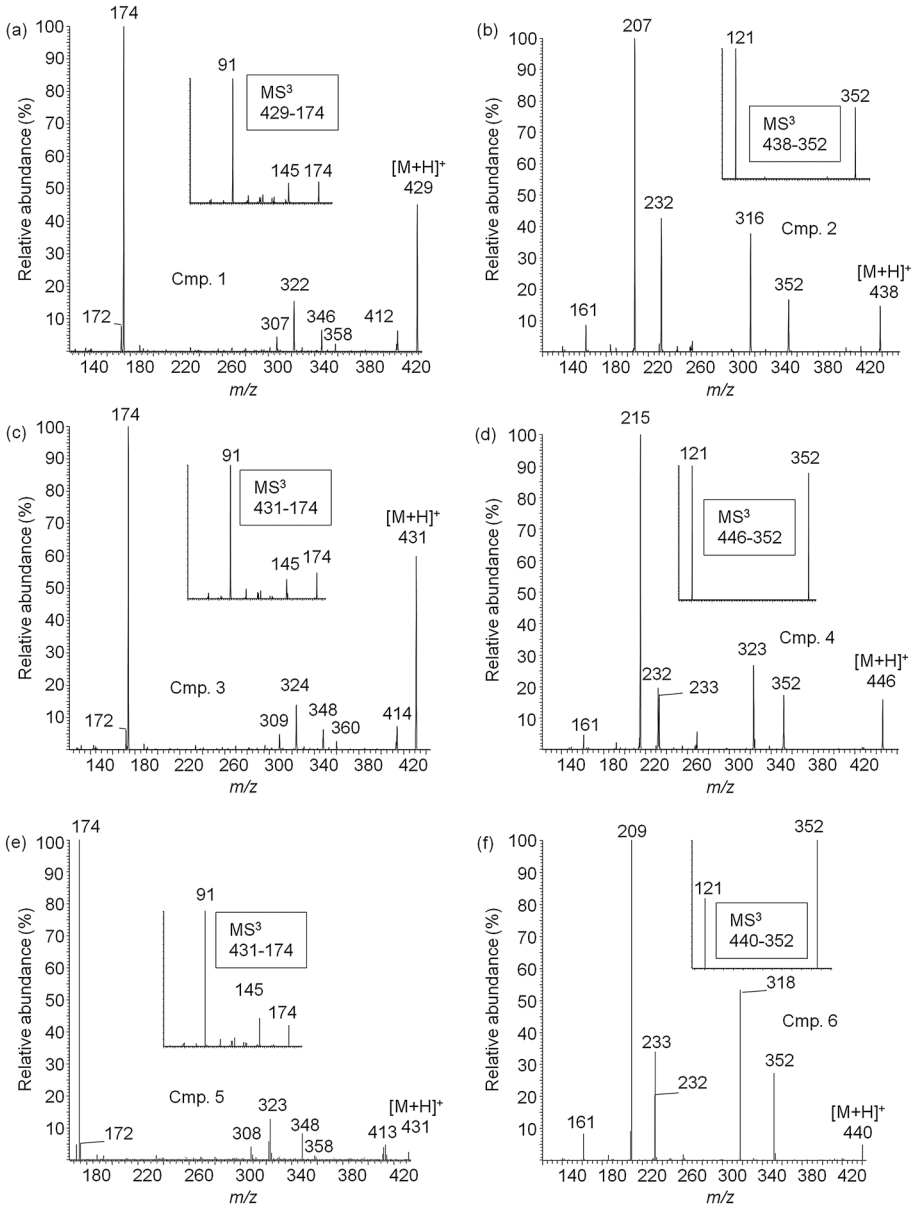

Figure 2. Electrospray ionization product ion mass spectra acquired in the linear ion trap (low resolution) of adipoR agonists **1** to **4** and corresponding spectra following H/D-exchange (**5** and **6**) measured on an LTQ Orbitrap (arbitrary units = a. u., collision energy = CE): a) AdipoRon (**1**), CE = 23 a. u.; b) $^{13}C_2$-AdipoRon (**3**), CE = 23 a. u.; c) 112254 (**2**), CE = 20 a. u.; d) D_8-112254 (**4**), CE = 20 a. u.; e) compound **5**, CE = 23 a. u.; f) compound **6**, CE = 23 arbitrary units. Spectra of MS^3 experiments are shown as inserts in MS/MS product ion spectra.

The loss of ammonia (17 u) from the protonated molecule of **1** leads to *m/z* 412 and, subsequently, the elimination of two ethine units (in sum 54 u) yields the product ion at *m/z* 358 (Scheme 2a). The proposed route is supported by analyses of ISTD **3** and **1** following H/D-exchange (Fig. 2c/e), where both ^{13}C-labels were retained, and both introduced deuterium atoms were removed from the product ion during formation.

The second most abundant product ion (*m/z* 322) represents the result of the elimination of benzylamine (Scheme 2d). Also here, supporting evidence is provided by the labeled ISTD (**3**, Fig. 2c) and compound **5** (Fig. 2e), demonstrating the presence of two ^{13}C- and one deuterium label.

An unusual ion was formed from the protonated molecule of **1** with the product observed at *m/z* 346. With the elemental composition of $C_{22}H_{20}NO_3$ it is suggested that the entire piperidine ring is intramolecularly eliminated and the benzyl residue rearranged to connect to the amide nitrogen (Scheme 2c). Several examples for intramolecular elimination reactions under CID conditions are given in the literature such as, e.g. the elimination of SO_2 in thiazide-based diuretics.[26] The difference, however, is that such elimination reactions were observed to occur when (intermediately formed) cyclic systems were available. In the present case, equilibrium structure determined by DTF calculation (Fig. 3a) does not suggest any cyclic structure; nevertheless, the release of the tetrahydropyridine residue is undisputed and corroborated by the product ion at *m/z* 348 of both the labeled AdipoRon **3** (Fig. 2c) and compound **5** as a result of H/D exchange (Fig. 2e). In order to elucidate the underlying mechanism, further studies are required.

The product ion at *m/z* 105, assigned to positively charged benzaldehyde, was shown to be generated from both *m/z* 346

Journal of MASS SPECTROMETRY

Table 1. Elemental composition of protonated molecules of **1** to **6** and product ions (>5% of relative abundance) using high-resolution/high mass accuracy MS^n experiments acquired on an LTQ Orbitrap

Compound	Precursor ion (*m/z*)	Elemental composition (exp.)	Error [ppm]	Collision energy [arb. units]	Product ion (*m/z*) (exp)	Elemental composition (exp.)	Error [ppm]	Cleaved species
AdipoRon (**1**)	429.2164	$C_{27}H_{29}N_2O_3$	−1.99	35	412.1895	$C_{27}H_{26}NO_3$	−3.00	NH_3
				35	358.1426	$C_{23}H_{20}NO_3$	−3.22	C_4H_6
				35	346.1431	$C_{22}H_{20}NO_3$	−2.04	C_5H_9N
				35	322.1433	$C_{20}H_{20}NO$	−1.52	C_7H_9N
				35	307.1797	$C_{20}H_{23}N_2O$	−2.58	$C_7H_6O_2$
				35	174.1275	$C_{12}H_{16}N$	−1.46	$C_{15}H_{13}NO_3$
				35	172.1119	$C_{12}H_{14}N$	−1.18	$C_{15}H_{15}NO_3$
				35	105.0377	C_7H_5O	2.04	$C_{13}H_{15}NO_2$
				35	91.0544	C_7H_7	2.13	C_5H_9N
112254 (**2**)	438.2748	$C_{26}H_{36}N_3O_3$	−0.75	20	352.1905	$C_{22}H_{26}NO_3$	−0.64	$C_4H_{10}N_2$
				20	316.2016	$C_{18}H_{26}N_3O_2$	−1.09	$C_8H_{10}O$
				20	232.1329	$C_{14}H_{18}NO_2$	−1.32	$C_{12}H_{18}N_2O$
				20	207.1490	$C_{12}H_{19}N_2O$	−1.04	$C_{14}H_{17}NO_2$
				20	161.0959	$C_{11}H_{13}O$	−0.89	$C_7H_{13}N_3O$
				20	121.0648	C_8H_9O	−0.18	$C_4H_{10}N_2$
$^{13}C_2$-AdipoRon (**3**)	431.2235	$C_{25}^{13}C_2H_{29}N_2O_3$	−1.03	35	414.1969	$C_{25}^{13}C_2H_{26}NO_3$	−1.18	NH_3
				35	360.1502	$C_{21}^{13}C_2H_{20}NO_3$	−0.83	C_4H_6
				35	348.1501	$C_{20}^{13}C_2H_{20}NO_3$	−1.04	C_5H_9N
				35	324.1501	$C_{18}^{13}C_2H_{20}NO_3$	−1.30	C_7H_9N
				35	309.1861	$C_{18}^{13}C_2H_{23}N_2O$	−1.27	$C_7H_6O_2$
				35	174.1276	$C_{12}H_{16}N$	−0.98	$C_{13}^{13}C_2H_{13}NO_3$
				35	172.1119	$C_{12}H_{14}N$	−0.80	$C_{13}^{13}C_2H_{15}NO_3$
				35	105.0337	C_7H_5O	2.42	$C_{11}^{13}C_2H_{15}NO_2$
				35	91.0546	C_7H_7	3.89	$C_3^{13}C_2H_9N$
D_8-112254 (**4**)	446.3247	$C_{26}H_{28}D_8N_3O_3$	−1.53	20	352.1904	$C_{22}H_{26}NO_3$	−0.82	$C_4H_2D_8N_2$
				20	323.2455	$C_{18}H_{19}D_7N_3O_2$	−1.11	C_8H_9DO
				20	232.1330	$C_{14}H_{18}NO_2$	−0.95	$C_{12}H_{10}D_8N_2O$
				20	233.1395	$C_{14}H_{17}DNO_2$	−0.04	$C_{12}H_{11}D_7N_2O$
				20	215.1993	$C_{12}H_{11}D_8N_2O$	−0.67	$C_{14}H_{17}NO_2$
				20	161.0960	$C_{11}H_{13}O$	−0.62	$C_7H_6D_7N_3O$
				20	121.0648	C_8H_9O	0.15	$C_4H_2D_8N_2$
D_2-AdipoRon (**5**)	431.2288	$C_{27}H_{27}D_2N_2O_3$	−2.29	35	413.1960	$C_{27}H_{25}DNO_3$	−2.34	NH_2D
				35	358.1427	$C_{23}H_{20}NO_3$	−2.99	C_4H_5D
				35	359.1484	$C_{23}H_{19}DNO_3$	−4.61	C_4H_8N
				35	348.1554	$C_{22}H_{18}D_2NO_3$	−0.88	C_5H_9N
				35	323.1493	$C_{20}H_{19}DNO$	−2.20	C_7H_8DN
				35	308.1861	$C_{20}H_{22}DN_2O$	−0.61	$C_7H_5DO_2$
				35	174.1270	$C_{12}H_{16}N$	−1.47	$C_{15}H_{11}D_2NO_3$
				35	172.1119	$C_{12}H_{14}N$	−1.19	$C_{15}H_{13}D_2NO_3$
				35	105.0337	C_7H_5O	1.62	$C_{13}H_{14}DNO_2$
				35	91.0545	C_7H_7	3.14	C_5H_9N
D_2-112254 (**6**)	440.2867	$C_{26}H_{34}D_2N_3O_3$	−2.14	20	352.1900	$C_{22}H_{26}NO_3$	−1.93	$C_4H_8D_2N_2$
				20	318.2016	$C_{18}H_{24}D_2N_3O_2$	−1.95	$C_8H_{10}O$
				20	232.1329	$C_{14}H_{18}NO_2$	−1.47	$C_{12}H_{16}D_2N_2O$
				20	233.1392	$C_{14}H_{17}DNO_2$	−1.28	$C_{12}H_{17}D_1N_2O$
				20	209.1615	$C_{12}H_{17}D_2N_2O$	−1.25	$C_{14}H_{17}NO_2$
				20	161.0958	$C_{11}H_{13}O$	−1.55	$C_7H_{11}N_3O$
				20	121.0648	C_8H_9O	−0.23	$C_4H_8D_2N_2$

(−241 u) and *m/z* 322 (−217 u, Scheme 2c/d, Table 1) as identified MS^3 experiments.

*112254 (**2**)*

DFT computation of 112254 yielded highest proton affinities of the molecule at the nitrogen of the piperazine moiety (position 18) as well as the carbonyl-oxygen at position 15. The equilibrium structures are shown in Figs. 3b and 3c, respectively, and despite substantially different three-dimensional features, the protonation at position 18 (nitrogen) is only favored by 3 kJ/mol^{-1}. Hence, both locations are considered as similarly preferred as initial ionization sites. Under CID conditions, the predominant product ion of the protonated molecule of **2** is *m/z* 207, suggested to represent the

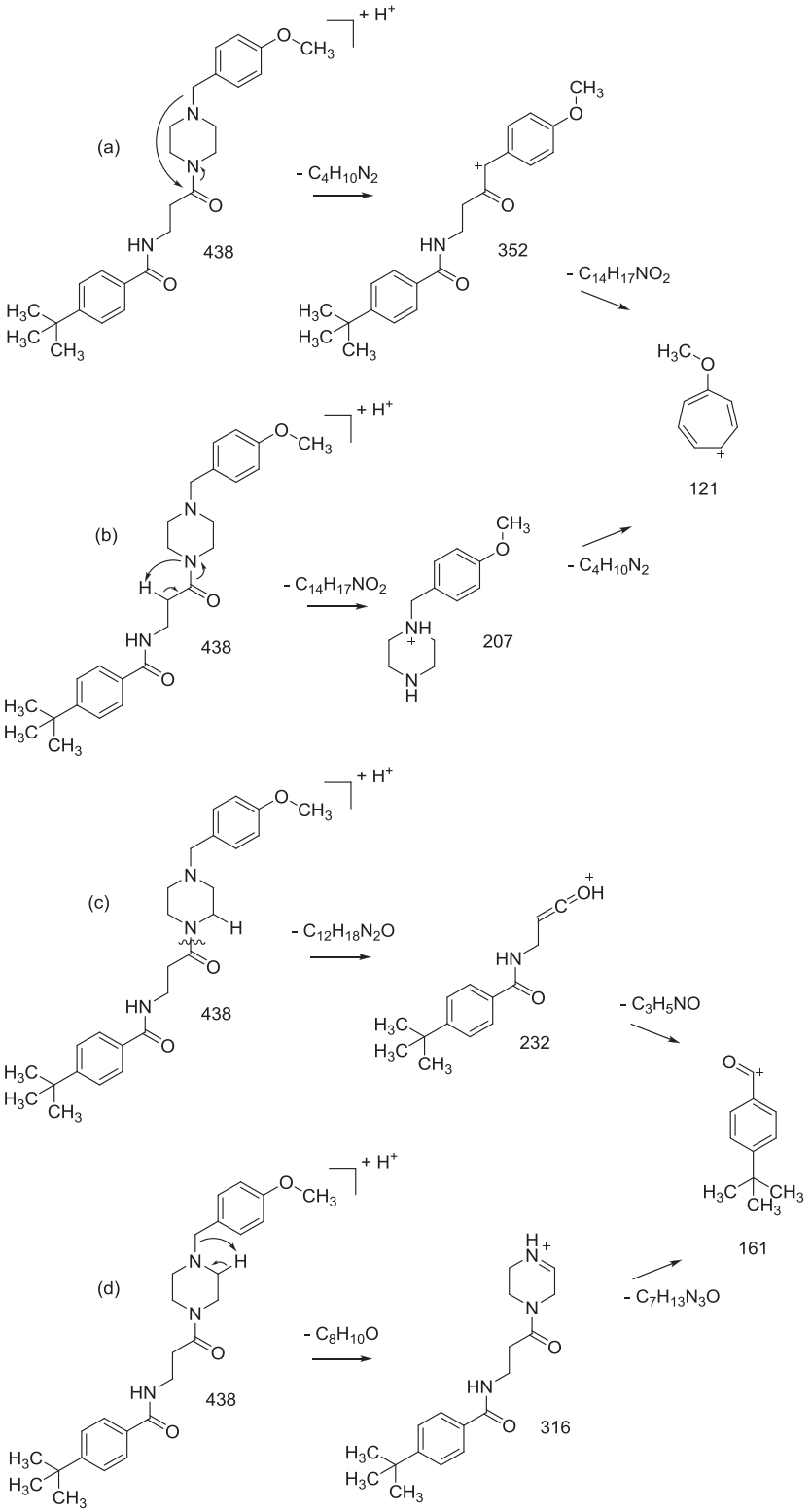

Scheme 3. Proposed dissociation pathway of 112254 (**2**).

protonated 1-(4-methoxybenzyl)piperazine as presumably generated by cleavage of the bond between position 15 and 21 (231 u, Scheme 3b). This ion is confirmed both by the protonated labeled ISTD **4** (Fig. 2d), where the eight deuterium atoms are retained, and by the H/D exchange experiment (**6**, Fig. 2f), where the two hydrogen atoms attached to the piperazine ring are substituted by deuterium.

By analogy with AdipoRon (**1**), the protonated molecule of **2** forms the product ion at *m/z* 352, suggesting that the piperazine ring is expelled per intramolecular elimination (−86 u, Scheme 3a).

Journal of MASS SPECTROMETRY

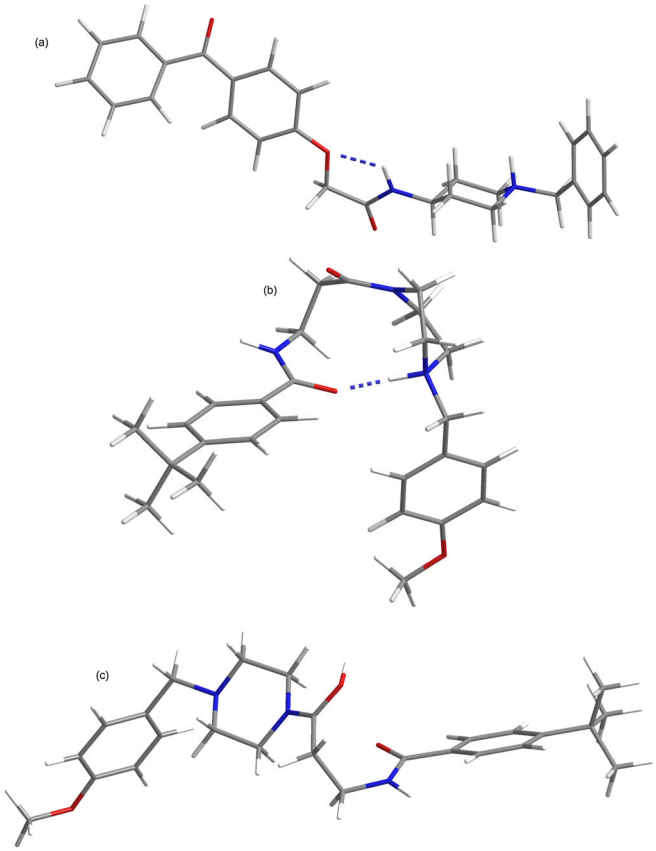

Figure 3. Equilibrium structures after DFT calculation (grey: carbon, white: hydrogen, red: oxygen, blue: nitrogen, dashed line: hydrogen bond): a) AdipoRon (**1**) protonated at position 21; b) 112254 (**2**) protonated at position 18; c) 112254 (**2**) protonated at position 15.

In case of 112254 (**2**), some details are of considerable interest and result from the fact that all protonated molecules of **2**, the labeled ISTD **4,** and compound **6** (H/D experiment) yield a product ion at *m/z* 352 (Figs. 2b/d/f). It appears plausible that the entire piperazine moiety is eliminated since no deuterium atom of compound **4** remains in the charged species at *m/z* 352. Also, the deuterium at the nitrogen in position 12 of **6** is replaced by hydrogen during the dissociation process. Since this hydrogen must have its origin in the molecule itself, the elimination route is likely to necessitate a more complex mechanism than depicted in Scheme 3a, and a cyclic transition state is probable, especially as the protonated molecule of **2** can be 'folded' due to the formation of a hydrogen bond as illustrated in Fig. 3b. In MS^3 experiments, both *m/z* 352 (−231 u) and *m/z* 207 (−86 u) yield the methoxycycloheptatrienyl cation *m/z* 121 (Fig. 2b, Scheme 3a/b).

Another interesting product ion is *m/z* 232. It is suggested that, if the protonation occurs at the oxygen in position 15 (Fig. 3c), a neutral loss of the 1-(4-methoxybenzyl)piperazine accompanied by a hydrogen shift from position 12, 13 or 14 towards the leaving group follows. Alternatively, if the initial protonation is at position 18 (Fig. 3b), a McLafferty-like rearrangement can contribute to a charge transfer from the piperazine residue to the carbonyl moiety, followed by the aforementioned elimination of 1-(4-methoxybenzyl)piperazine to form the ion at *m/z* 232 (Scheme 3c). These postulated pathways are supported by product ions at *m/z* 232 and *m/z* 233 obtained from the protonated molecule of the isotopically labeled compound **4** (Fig. 2d) bearing 8 deuterium atoms in the piperazine residue. Moreover, DFT calculations favored both protonation sites and resulting structures (Fig. 3b/c) equally, which is reflected by the identical relative abundances of the two product ions as shown in Fig. 2d.

The product ion at *m/z* 316 as formed from the protonated molecule of **2** is proposed to be generated by the elimination of 1-methoxy-4-methylbenzene (Scheme 3d). This structure is corroborated by both the protonated labeled ISTD **4** (Fig. 2d), where seven deuteriums are left at *m/z* 323 and by the H/D exchange experiment (**6**, Fig. 2f), where the hydrogen attached at the piperazine ring and the hydrogen of the amide bond are substituted by deuterium.

Both *m/z* 232 (−71 u) and *m/z* 316 (−155 u) yield a positively charged 4-(*tert*-butyl)benzaldehyde with *m/z* 161 in MS^3 experiments (Scheme 3c/d).

Assay validation

An assay for the qualitative determination of compounds **1** and **2** was established and validated for doping control purposes. Results are summarized in Table 2, and typical extracted ion chromatograms and corresponding mass spectra are illustrated in Fig. 4. In the absence of authentic administration study samples, only spiked specimens were used to provide proof-of-concept data, and the applicability of the developed methodology was demonstrated by common validation and method characterization parameters as outlined below.

Specificity

At expected retention times, no interfering signals were observed for both target analytes (**1**, **2**, Fig. 4a)

Lower limit of detection

Both AdipoRon (**1**) and 112254 (**2**) were identified at an estimated LLOD of 1 ng/ml (Table 2). As mentioned before, the maximal plasma concentration of AdipoRon (**1**) in mice found after oral administration (50 mg/kg^{-1} body weight) was 11.8 μM (5.1 mg/ml^{-1}) after 2 h.[16] This is considerably more than the found LLOD. To the best of our knowledge, no other studies have been published about pharmacokinetic or pharmacodynamic data yet but substantially lower plasma values are expected in humans. Hence, best possible sensitivity is desirable for sports drug testing purposes.

Table 2. Summary of assay validation results

Compound	LLOD [ng/ml]	Recovery [%] at 50 ng/ml	Ion suppression [%]
1	1	89	26
2	1	86	<10
	Precision:	Intraday precision ($n = 18$)	Interday precision ($n = 54$)
Compound	Concentration [ng/ml]	CV [%]	CV [%]
1	1	14–18	16
	50	3–6	7
	200	6–7	6
2	1	16–17	12
	50	4–7	5
	200	4–8	6

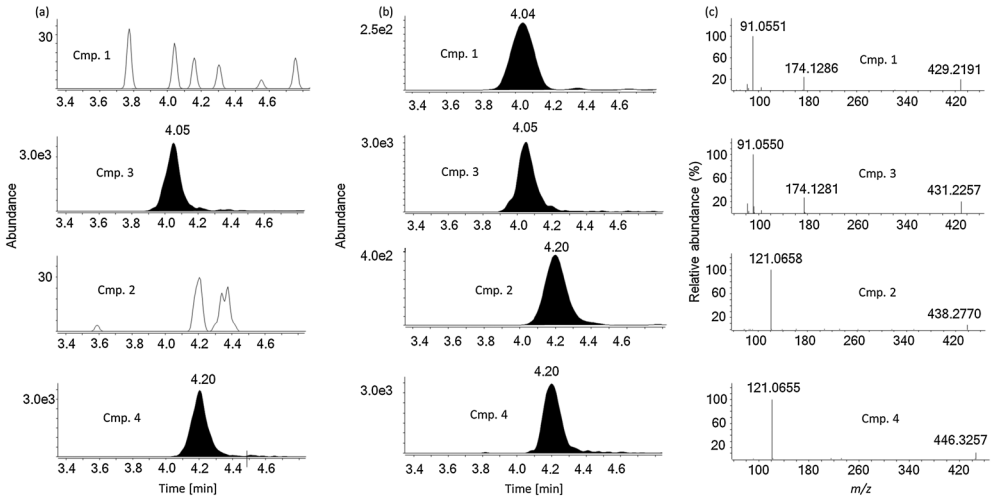

Figure 4. Extracted ion chromatograms of a) blank plasma containing both ISTDs (**3**, **4**) only; b) AdipoRon (**1**), precursor: $[M+H]^+ = 429.2173$, targeted product ion: *m/z* 91.0542; $^{13}C_2$-AdipoRon (**2**), precursor: $[M+H]^+ = 431.2240$, targeted product ion: *m/z* 91.0542; 112254 (**3**), precursor: $[M+H]^+ = 438.2751$, targeted product ion: *m/z* 121.0648; D_8-112254 (**3**), precursor: $[M+H]^+ = 446.3253$, targeted product ion: *m/z* 121.0648; all at 1 ng/ml; c) product ion mass spectra ($HRMS^2$) of all measured analytes.

Identification capability

The requirement for the identification capability, the retention time of the analyte shall not differ more than ±0.1 min, is fulfilled for both analyte **1** and **2**.

Robustness

The method's robustness was demonstrated by employing a different HPLC column and packing material with slightly different dimensions, which did not negatively influence peak resolution or peak form.

Carryover

At 200 ng/ml, a marginal carryover of 0.6% for AdipoRon (**1**) and 0.1% for 112254 (**2**) were determined. For lower concentrations, no carryover was observed.

Matrix interference

Four plasma samples were prepared and analyzed as described. For AdipoRon (**1**) an ion suppression of 26% was determined. 112254 (**2**) has shown an ion suppression of less than 10% at expected retention time (Table 2).

Recovery

The recovery was determined to be 89% for AdipoRon (**1**) and 86% for 112253 (**3**) as shown in Table 2.

Intraday and interday precision

Intraday and interday precision were determined at three concentrations of both target analytes (**1**, **2**). They range from 14% to 18% for low concentration (1 ng/ml), from 3% to 7% for medium concentration (50 ng/ml) and from 4% to 8% for high concentration (200 ng/ml) as shown in Table 2.

Linearity

For both AdipoRon (**1**) and 112254 (**2**) a linear approximation yielded a coefficient of correlation of R = 0.99 for 1–200 ng/ml.

Conclusion

Preventive doping research is a crucial method to incorporate new, emerging drugs into sports drug testing as soon as a potential abuse of new therapeutics can be anticipated. An impediment is the availability of the new drugs. Reference material is crucial to establish reliable and sensitive detection assays. Since novel substances, especially in early stages of development, are not readily available, chemical synthesis and full characterization are necessary.

In the present study, adipoR agonists belonging to a new substance class based on the adipokine adiponectin were prepared and implemented in doping control procedures as these therapeutics might possess potential for misuse due to their capability to increase the mitochondrial content in muscle cells. Two compounds and two corresponding labeled analogs of this substance class were synthesized, fully characterized by NMR, DFT computation and mass spectrometry, and a test method was validated for human plasma. The data obtained will be available for future *in vitro*/*in vivo* studies, the identification of metabolites and the development of an analytical assay to detect these compounds in urine.

Acknowledgements

The project was supported by Anti-Doping Switzerland (Berne, Switzerland), the German Federal Ministry of the Interior and the Manfred-Donike-Institute for Doping Analysis (Cologne, Germany).

References

[1] E. Hu, P. Liang, B. M. Spiegelman. AdipoQ is a novel adipose-specific gene dysregulated in obesity. *J. Biol. Chem.* **1996**, *271*, 10697.
[2] K. Maeda, K. Okubo, I. Shimomura, T. Funahashi, Y. Matsuzawa, K. Matsubara. cDNA Cloning and Expression of a Novel Adipose Specific Collagen-like Factor, apM1 (AdiposeMost Abundant Gene Transcript 1). *Biochem.Biophys. Res. Com.* **1996**, *221*, 286.
[3] T. Tobe, N. H. Choi-Miura, T. Mazda, M. Tomita. Isolation and characterization of GBP28, a novel gelatin-binding protein purified from human plasma. *J. Biochem.* **1996**, *120*, 803.
[4] P. E. Scherer, S. Williams, M. Fogliano, G. Baldini, H. F. Lodish. A Novel Serum Protein Similar to C1q, Produced Exclusively in Adipocytes. *J. Biol. Chem.* **1995**, *270*, 26746.

[5] Y. Arita, S. Kihara, N. Ouchi, M. Takahashi, K. Maeda, J.-i. Miyagawa, K. Hotta, I. Shimomura, T. Nakamura, K. Miyaoka, H. Kuriyama, M. Nishida, S. Yamashita, K. Okubo, K. Matsubara, M. Muraguchi, Y. Ohmoto, T. Funahashi, Y. Matsuzawa. Paradoxical Decrease of an Adipose-Specific Protein, Adiponectin, in Obesity. *Biochem. Biophys. Res. Co.* **1999**, *257*, 79.
[6] T. Yamauchi, J. Kamon, Y. Ito, A. Tsuchida, T. Yokomizo, S. Kita, T. Sugiyama, M. Miyagishi, K. Hara, M. Tsunoda, K. Murakami, T. Ohteki, S. Uchida, S. Takekawa, H. Waki, N. H. Tsuno, Y. Shibata, Y. Terauchi, P. Froguel, K. Tobe, S. Koyasu, K. Taira, T. Kitamura, T. Shimizu, R. Nagai, T. Kadowaki. Cloning of adiponectin receptors that mediate antidiabetic metabolic effects. *Nature* **2003**, *423*, 762.
[7] T. Kadowaki, T. Yamauchi. Adiponectin and adiponectin receptors. *Endocr. Rev.* **2005**, *26*, 439.
[8] T. Yamauchi, J. Kamon, H. Waki, Y. Terauchi, N. Kubota, K. Hara, Y. Mori, T. Ide, K. Murakami, N. Tsuboyama-Kasaoka, O. Ezaki, Y. Akanuma, O. Gavrilova, C. Vinson, M. L. Reitman, H. Kagechika, K. Shudo, M. Yoda, Y. Nakano, K. Tobe, R. Nagai, S. Kimura, M. Tomita, P. Froguel, T. Kadowaki. The fat-derived hormone adiponectin reverses insulin resistance associated with both lipoatrophy and obesity. *Nat. Med.* **2001**, *7*, 941.
[9] A. H. Berg, T. P. Combs, X. Du, M. Brownlee, P. E. Scherer. The adipocyte-secreted protein Acrp30 enhances hepatic insulin action. *Nat. Med.* **2001**, *7*, 947.
[10] T. Yamauchi, J. Kamon, Y. Minokoshi, Y. Ito, H. Waki, S. Uchida, S. Yamashita, M. Noda, S. Kita, K. Ueki, K. Eto, Y. Akanuma, P. Froguel, F. Foufelle, P. Ferre, D. Carling, S. Kimura, R. Nagai, B. B. Kahn, T. Kadowaki. Adiponectin stimulates glucose utilization and fatty-acid oxidation by activating AMP-activated protein kinase. *Nat. Med.* **2002**, *8*, 1288.
[11] B. B. Kahn, T. Alquier, D. Carling, D. G. Hardie. AMP-activated protein kinase: ancient energy gauge provides clues to modern understanding of metabolism. *Cell Metab.* **2005**, *1*, 15.
[12] T. Yamauchi, Y. Nio, T. Maki, M. Kobayashi, T. Takazawa, M. Iwabu, M. Okada-Iwabu, S. Kawamoto, N. Kubota, T. Kubota, Y. Ito, J. Kamon, A. Tsuchida, K. Kumagai, H. Kozono, Y. Hada, H. Ogata, K. Tokuyama, M. Tsunoda, T. Ide, K. Murakami, M. Awazawa, I. Takamoto, P. Froguel, K. Hara, K. Tobe, R. Nagai, K. Ueki, T. Kadowaki. Targeted disruption of AdipoR1 and AdipoR2 causes abrogation of adiponectin binding and metabolic actions. *Nat. Med.* **2007**, *13*, 332.
[13] M. Iwabu, T. Yamauchi, M. Okada-Iwabu, K. Sato, T. Nakagawa, M. Funata, M. Yamaguchi, S. Namiki, R. Nakayama, M. Tabata, H. Ogata, N. Kubota, I. Takamoto, Y. K. Hayashi, N. Yamauchi, H. Waki, M. Fukayama, I. Nishino, K. Tokuyama, K. Ueki, Y. Oike, S. Ishii, K. Hirose, T. Shimizu, K. Touhara, T. Kadowaki. Adiponectin and AdipoR1 regulate PGC-1alpha and mitochondria by Ca(2+) and AMPK/SIRT1. *Nature* **2010**, *464*, 1313.
[14] T. Kadowaki, T. Yamauchi, M. Iwabu, M. Iwabu, K. Touhara. Screening method for candidate agonist compounds for adiponectin receptor 1. International Patent EP 2 548 969, **2013**.
[15] T. Kadowaki, T. Yamauchi, M. Iwabu, M. Iwabu. Pharmaceutical for pseudo-exercise therapy. International Patent WO2011/115106 A1, **2013**.
[16] M. Okada-Iwabu, T. Yamauchi, M. Iwabu, T. Honma, K. Hamagami, K. Matsuda, M. Yamaguchi, H. Tanabe, T. Kimura-Someya, M. Shirouzu, H. Ogata, K. Tokuyama, K. Ueki, T. Nagano, A. Tanaka, S. Yokoyama, T. Kadowaki. A small-molecule AdipoR agonist for type 2 diabetes and short life in obesity. *Nature* **2013**, *503*, 493.
[17] W. L. Holland, P. E. Scherer. Cell Biology. Ronning after the adiponectin receptors. *Science* **2013**, *342*, 1460.
[18] World Anti-Doping Agency. The 2014 Prohibited List International Standard Version 2.0. Available at: https://wada-main-prod.s3.amazonaws.com/resources/files/WADA-Revised-2014-Prohibited-List-EN.PDF, accessed 29. August 2014.
[19] N. L. Allinger. Conformational analysis. 130. MM2. A hydrocarbon force field utilizing V1 and V2 torsional terms. *J. Am. Chem. Soc.* **1977**, *99*, 8127.
[20] Max-Plank-Institute for Chemical Energy Conversion. ORCA - An ab initio, DFT and semiempirical SCF-MO package. Available at: https://cec.mpg.de/forum/portal.php, accessed 24. July 2014.
[21] J. P. Perdew, K. Burke, M. Ernzerhof. Generalized Gradient Approximation Made Simple. *Phys. Rev. Lett.* **1996**, *77*, 3865.
[22] F. Weigend, M. Häser, H. Patzelt, R. Ahlrichs. RI-MP2: optimized auxiliary basis sets and demonstration of efficiency. *Chem. Phys. Lett.* **1998**, *294*, 143.
[23] World Anti-Doping Agency. International Standard for Laboratories Available at: https://wada-main-prod.s3.amazonaws.com/resources/files/WADA-ISL-2015-Final-v8.0-EN.pdf, accessed 14. October 2014.
[24] World Anti-Doping Agency. Identification Criteria for qualitative Assays. Available at: https://wada-main-prod.s3.amazonaws.com/resources/files/WADA_TD2010IDCRv1.0_Identification%20Criteria%20for%20Qualitative%20Assays_May%2008%202010_EN.doc.pdf, accessed 14. October 2014.
[25] A. Kromidas, *Validierung in der Analytik*, Wiley-VCH: Weinheim, **1999**.
[26] M. Thevis, M. H. Schmickler, W. Schänzer. Mass spectrometric behavior of thiazide-based diuretics after electrospray ionization and collision-induced dissociation. *Anal. Chem.* **2002**, *74*, 3802.

